Low-cost solar PV soiling sensor validation and size resolved soiling impacts: A comprehensive field study in Western India

Michael Valerino[a,*], Mike Bergin[a], Chinmay Ghoroi[b], Aniket Ratnaparkhi[b], Greg P. Smestad[c]

[a] Civil and Environmental Engineering Department, Pratt School of Engineering, Duke University, Durham, NC 27705, USA
[b] DryProTech Lab, Chemical Engineering, India Institute of Technology Gandhinagar, Palaj, Gandhinagar, Gujarat 382355, India
[c] Sol Ideas Technology Development, P.O. Box 5729, San José, CA 95150, USA

ABSTRACT

Deposition of particulate matter (PM) onto solar photovoltaic (PV) panels - known as soiling - has been estimated to reduce energy production by 10–40% in many regions of the world. Despite this, many key properties including soiling rates, PM source contributions, physical and optical properties of the deposited particles, and the impact of rain and relative humidity (RH) are not well understood. With this in mind we conducted a field study in Gandhinagar, India. Our approach combines soiling monitoring with a reference station and a low-cost digital microscopy system, sample collection for mass loading information, glass sample slides for size resolved soiling impacts, and monitoring of rain, RH, and panel temperature for insight into meteorological impacts on cleaning and soiling rates. Results indicate soiling reduces PV energy production by $0.37 \pm 0.09\%$ day^{-1}. The low cost (< 100\$) digital microscope estimated soiling within ~1% of measured losses, confirming the feasibility of this low-cost alternative to expensive soiling stations. Deposited PM decreased energy production by $5.12 \pm 0.55\%$ per PM mass loading (g m^{-2}). Microscopy analyses of field samples revealed that > 90% of deposited mass loading is from particles > 5 μm in diameter, with > 50% of the soiling impacts estimated to be from particles < 5 μm. While heavy rain cleaned PV panels, light rains and high RH contributed to a 2x soiling rate and 5-10x PM deposition velocities as compared to dry periods.

1. Introduction

In developing countries, solar photovoltaic (PV) power represented the largest renewable energy investment at 57.5 billion USD in 2016 (REN21, 2018). India has a projected goal of 100 GW (GW) of PV by 2022. Dust and particulate matter (PM) deposition on solar panels - known as soiling - has been shown to reduce PV energy production by as much as 10 – 40% in a matter of weeks (Bergin et al., 2017). With influence from wind-blown dust in the dry seasons and anthropogenic PM emissions year-round, India is a region of focus for PV soiling studies. Gujarat in particular has a high potential for PV installations, and the soiling in the region represents much of Western India (Mahtta et al., 2014; Ramachandra et al., 2011).

While India is on the forefront of creating new solar installations, there is a lack of valuable soiling information available for the determination of performance ratios, maintenance budgeting, and location feasibility. Soiling impacts are often inaccurately lumped into 'losses' during evaluations (Dobaria et al., 2016; Khan and Rathi, 2014;

Padmavathi and Daniel, 2013; Shukla et al., 2016; Sundaram et al., 2015; Sharma and Chandel, 2016). A key reason for the lack of reliable soiling information is the expensive cost of soiling monitoring equipment. There is a need for low-cost tools that can provide accurate insight into soiling effects. In addition, it would be very advantageous to combine soiling information with more detailed analysis of the deposited PM. Some work has been done in dusty regions regarding soiling losses per unit mass of deposited PM, with reported values ranging from 3 to 6% per g m^{-2} (Boyle et al., 2015; Boyle et al., 2013; Bergin et al., 2017). This important indicator of deposited particulate light extinction properties needs to be more carefully studied with particle size analysis considered. While other studies have looked into size dependent soiling impacts of deposited PM, both in the field (Tanesab et al., 2017; Roth and Pettit, 1980; Goossens, 2005) and in laboratory experiments (Cuddihy, 1980; El-Shobokshy and Hussein, 1992), no studies have combined size distribution analysis of field samples with theoretical and measured soiling impacts in this region. This analysis would allow for information on how various sources of PM

---

are impacting PV energy production. In addition, there is not a clear agreement in the field on how meteorological variables, including rain and relative humidity (RH), impact both soiling rates and post-deposition processes like natural cleaning and cementation.

With all of this in mind, we have developed a field-based approach that took place in Gandhinagar, Gujarat, India. We have combined traditional soiling monitoring using a Campbell Scientific Soiling Station with a low-cost digital microscope system which, to our knowledge, is a method that has never been validated. Soiling monitoring has been combined with two types of sample collection. Deposited PM has been collected from the surface of panels to determine mass loadings. To address the lack of size dependent soiling information, glass slide samples (on which PM naturally deposited), have been analyzed for the impact of particle size distribution on soiling. Finally, the influence of rain, RH, and ambient PM concentrations is considered. This comprehensive study looks to address gaps in regional soiling knowledge to allow energy producers to make more informed management decisions regarding mitigation of soiling (Tanesab et al., 2018; Baras et al., 2016; Abu-Naser, 2017; Dolan et al., 2015; Jones et al., 2016).

2. Material and methods

2.1. Study location

This study took place on the campus of the India Institute of Technology Gandhinagar (IITGN) in Gandhinagar, the capital of Gujarat, India. On an unobstructed rooftop of a building on the campus, monitoring and sample collection equipment was set up, maintained and run from September 1st 2018 to January 9th 2019. This period is split into 6 3-week sampling periods referred to as A (September 1 - September 26), B (September 27 - October 17), C (October 18 - November 7), D (November 8 - November 30), E (November 31 - December 19) and F (December 20 - January 9).

2.2. Soiling measurements

Data for determination of soiling loss were obtained by a Campbell Scientific SMP100 soiling station. This soiling station used two, 50 Watt polycrystalline solar panels facing due south at a tilt angle of 23° (latitude of Gandhinagar). The reference panel was cleaned nightly with a microfiber cleaning towel and deionized (DI) water, while PM naturally deposited on the soiled panel. A data logger (Campbell CR-PVS1) recorded short-circuit current (I_{sc}) output and module temperature of both at a five minute interval. I_{sc} was then multiplied by the open circuit voltage (V_{oc}) of the panel and the recording time interval (300 s) to obtain an estimated energy output in Joules. It should be noted this method is not the same as the IEC standard for soiling (IEC 61724). Although the fill factor (maximum power over the product of I_{sc} and V_{oc}) will be influenced by soiling, we assume a constant value that will be canceled out in the soiling loss calculation. This is defined by Eq. (1):

$$SL = \left(1 - \frac{E_{soiled}}{E_{reference}}\right) * 100\%$$

(1)

where *SL* is the soiling loss (%) for a given day, E_{soiled} is daily energy production of the soiled panel (J), and $E_{reference}$ is the daily energy production of the reference (cleaned) panel (J). It should be noted that temperature differences due to soiling are not accounted for in the soiling loss calculation, and are discussed later. The sensitivity of the temperature probe used is 0.15 °C.

Deposited PM was collected from the soiled panel surface (0.37 m^2) every 3 weeks. A corner of the solar panel frame was cut away to allow for deposited dust to be scraped off the panel with a Thomas Scientific Steriplast Scraper and into a sterile glass jar below the panel. All attempts were made to ensure that wind did not carry away dust as it was

being collected, including delaying collection until winds were low (< 1 m s^{-1}) and using an umbrella to block any remaining breeze. This dust collection method is similar to that described by Javed et al. (2017). The panel was then cleaned with DI water and a microfiber cloth to remove any remaining particles. The mass of the deposited PM was measured with a Mettler Toledo AG 245 balance (with a precision of $\pm$ 0.2 mg), with PM mass values ranging from 40 to 700 mg (mg).

2.3. Meteorological data

Meteorological data were recorded at five-minute intervals using a Campbell Scientific CR1000 datalogger. Meteorological data were needed for assessment of natural cleaning by rain and to assess the impact of humidity on soiling rates. Attached instrumentation included temperature and relative humidity (Campbell Scientific EE181-L probe), and a rain gauge (Texas Electronics TR-525I). To assess the impact of ambient PM on soiling, an inexpensive PM monitor (Zheng et al., 2018) was deployed. The monitor uses a low cost light scattering sensor (Plantower PMS3003) along with custom hardware and software for data collection and calibration. The sensor is accurate to ∼ 10% of ambient concentrations (Zheng et al., 2018).

2.4. Low cost digital microscope system

In order to fulfil the need for a low-cost system to estimate soiling, a digital microscope (Celestron Handheld Digital Microscope Pro 5MP) was used to capture daily images of deposited PM. The microscope had a low-iron glass slide (VWR Vistavision Unimark 75 × 25 × 1 mm) secured directly above the digital camera mounted on the camera stand, which was exposed to the air pointed due south at 23°tilt. Image analyses were done on images taken at 11PM when the microscope's internal LED lights illuminated particles against the dark night sky (see Supplemental Information for description of the system layout). Images taken with this microscope are ~2750 × 2070 μm. The setup was similar to that described by Figgis et al. (2016). The system was cleaned simultaneously to the Campbell Scientific station (every 3 weeks) with DI water and a microfiber cloth. Parameters described in subsequent sections with a 'dm' subscript will be used to indicate they were derived from this digital microscope method.

2.5. Optical microscope analyses

To determine size distribution and size dependent impacts of soiling, low iron, glass cover slips (VWR 22 × 22 mm No 1.5 – 0.16 to 0.19 mm in thickness) were used as sample slides for imaging deposited PM. These slides were secured to a custom 3D printed mount via a small rubber band. This mount and slide piece were then attached to another 3D printed bracket bolted to the side of a solar panel (See Supplementary Information for an image of the setup in the field). The glass slides were left out for a 3-week sampling period before being collected.

A Ziess Axio Observer microscope with a Hamamatsu Orca ER digital camera (1344 × 1024 pixels) was used to acquire micrographs of the field samples. Images to be used for determination of size distribution, mass loading estimations, and soiling loss estimations were taken with 20x and 100x objective lenses. The microscope eyepiece adds 10x magnification as well. Throughout this manuscript, '20x' and '100x' will be used to refer to the images taken through the 20x and 100x objective microscope lens. The dimension of the 20x images are ∼ 420 × 320 μm (1 pixel = 0.311 μm) and the 100x images are 84 × 64 μm (1 pixel = 0.063 μm). 20x images were taken at a 5x5 image grid, while 100x images were taken in a 3x3 grid. Analysis of the 100x images were used for particle diameters from 0.25 to 3 μm, while the 20x images were used for all larger particle sizes. Parameters described with an 'om' subscript indicate they were obtained from this optical microscopy method. See Supplementary Information for a more
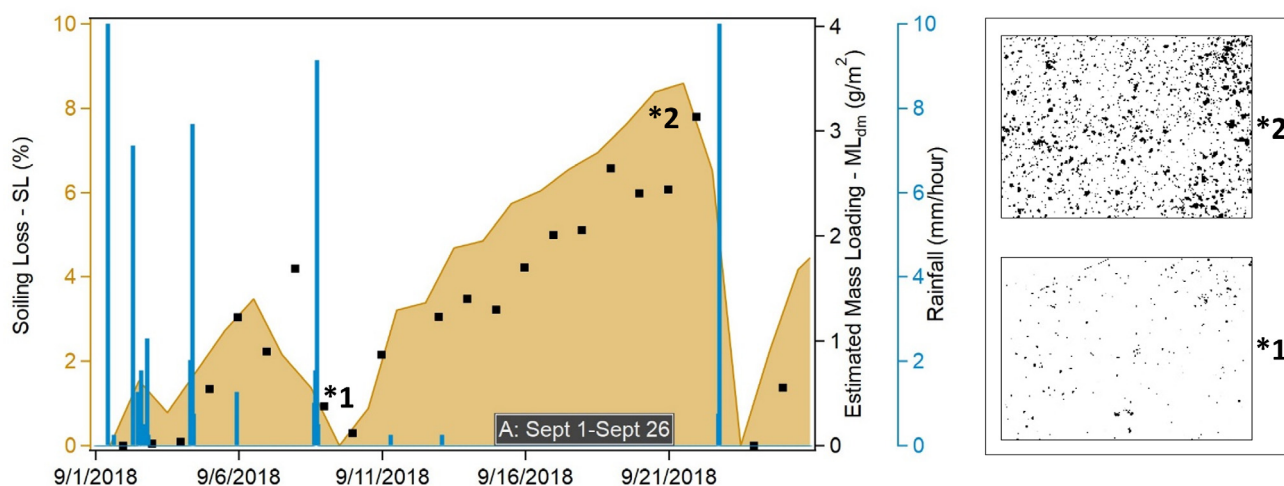
Fig. 1. The filled tan trace is the soiling measurement as recorded by the Campbell Scientific soiling station (SL). The square black points are the mass loading estimations acquired by the digital microscope (ML_{dm}). Vertical blue bars are rain amounts during events. For the two asterisked days (on September 2nd and September 21st) the corresponding processed image from the digital microscope is shown to the right where particles are black against a white background.

detailed image analysis procedure and examples of images taken with this microscope. To more closely analyze deposited PM, a scanning electron microscope (FEI XL30 SEM-FEG) was used with a 5 kV beam.

2.6. Mass loading estimations from microscopy images

Mass loadings were estimated from micrographs obtained from both the digital microscope system, and the optical microscope images of the sample slides. Mass, rather than another metric (i.e. surface area), was estimated to allow to comparison with literature values of mass loadings and soiling loss per unit mass. Mass estimations also allows for comparison with measured mass loadings in this study. To estimate mass loadings, particle size was determined through image analysis by the ImageJ software (Schindelin et al., 2012). Particles were then counted and separated by bin size. Bin sizing was determined with a balance between size resolution and statistical power in mind (See supplementary information for the bin sizing used). The mass loading of each bin size was found by the number of particles in that bin size, an assumed density of 1.6 g cm^{-3} - based on a study by Hu et al. (2012) - and an assumption of spherical particles. The mass loading of all bins was summed to determine total mass loading.

2.7. Soiling loss estimation

To determine soiling loss from images obtained via optical microscopy (SL_{om}), an optical model based on one developed by Bergin et al. (2017) was used. This is described by Eq. (2) which describes estimated losses by:

$$SL_{om} = (-100\%) \sum_{i=1}^{n} (E_{abs,i} + \beta_i E_{scat,i}) ML_{om,i},$$

(2)

where SL_{om} is the estimated soiling loss estimated from images obtained via optical microscopy, n = the number of size bins from 0.25 to 100 μm particle diameter, $E_{abs,i}$ is the mass absorption efficiency of size bin i, $E_{scat,i}$ is the scattering efficiency of size bin i, β_i is the backscatter fraction of bin i, and $ML_{om,i}$ is the mass loading of size bin i which is estimated from image analysis of the sample slides.

For the scattering and absorption efficiencies, Mie Theory (Mie, 1908) calculations were carried out at 550 nm wavelength (the peak of the solar spectrum) by the software MiePlot (Laven, 2018). In the Mie Theory calculations, the real part of the refractive index was assumed to be 1.5 and the imaginary part was 0.02, consistent with measured results from the region (Pandithurai et al., 2008). Particles above 5 μm

were assumed to be primarily mineral dust with an assumed absorption efficiency of 0.02 m^2 g^{-1}, consistent with wind-blown dust field measurements (Yang et al., 2009; Xu et al., 2002). The backscatter fraction was approximated from Wiscombe and Grams (1976). Though particles may not be spherical, this assumption should not influence Mie Theory calculations by more than 10% (Mishchenko et al., 1997). See the Supplementary Information for more detail on the soiling loss estimations and the development of the model given in Eq. (2).

3. Results and discussion

We first compare mass loading estimations from our novel digital microscopy method with the soiling results from a Campbell Scientific soiling reference station. We evaluate the low-cost microscopy method's ability to estimate daily soiling losses. We then provide size-resolved soiling estimations for insight into sources and removal strategies through the analysis of micrographs combined with an optical transmittance model. The threshold of natural cleaning by rain and the impact of RH and ambient PM on soiling rate and deposition velocity is then quantified. Finally, the effect of the difference in soiled versus unsoiled module temperature on panel efficiency is reported.

3.1. Observed soiling losses and mass loading estimations

Estimations of surface PM mass loadings were obtained using images recorded by the digital microscope system. Fig. 1 shows the processed images with the associated mass loading estimation, together with measured soiling loss and rainfall for sampling period A (September 1st to 26th, 2018). Mass loading estimations from the digital microscope system are referred to as ML_{dm}, where the 'dm' subscript stands for digital microscopy and measured soiling loss as recorded by the Campbell Scientific soiling station is SL.

The heavy (> 8mm h^{-1}) rain events on September 8th and September 22nd restored panels to less than 0.1% soiling loss. Despite the rain, soiling loss (filled tan trace of Fig. 1) increased continuously during dry periods. This suggests continued mass accumulation, which is confirmed by the digital microscope images and associated mass loading estimations. The light coating of particles (that appear black on the images) seen on September 2nd (*1) yielded a ML_{dm} estimation of 0.02 g m^{-2}, several orders of magnitude less than the 3.14 g m^{-2} estimated from the September 21st image (*2), which is seen to have a thick coating of particles present. This highlights the ability of the approach to estimate a broad range of mass loadings.
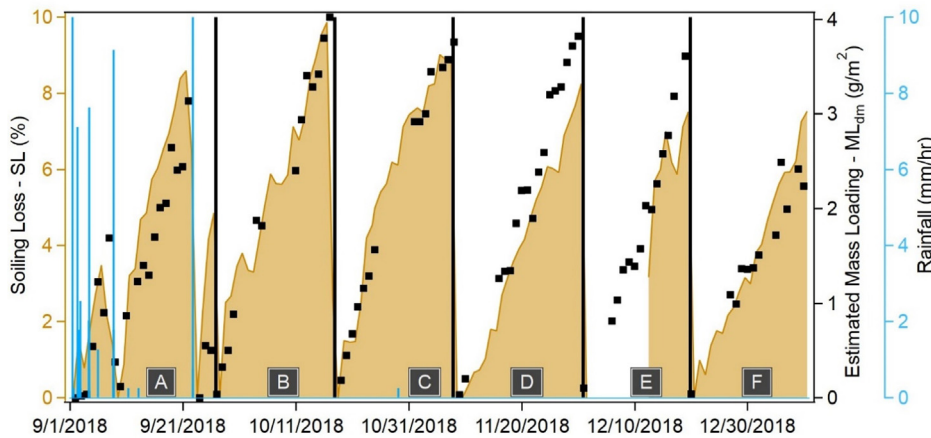
Fig. 2. Soiling results (filled tan trace) are compared against rain data (vertical light blue bars) and microscopy image analysis estimates of mass loading (square black points) for 6, 3-week sampling periods. The systems were monitored and maintained from 9/1/2018 to 1/9/2019 on the campus of IIT Gandhinagar. The system did not record from 12/1 to 12/12 and vertical black lines represent cleaning days.

Fig. 2 shows the extension of this plot for all 6 sampling periods (A-F). Throughout the six sampling periods, the Pearson Correlation Coefficient between ML_{dm} and SL was found to be 0.83. This significant, positive relationship between ML_{dm} and SL, despite variable soiling due to rain events, indicates the ability of the digital microscopy system to estimate mass loadings that are statistically correlated with soiling loss.

PM continued to accumulate on the PV panels throughout the study (ML_{dm}) and the soiling loss (SL) response was $8.0 \pm 1.6\%$ over 3 weeks (0.37% day^{-1}), with the relatively small coefficient of variation (20%). This indicates that the soiling rate remained similar over the time periods of sampling. Information on soiling rate is necessary to determine cleaning schedules and generate performance models, both of which are crucial to maximizing energy production and economic feasibility of a PV system (Jones et al., 2016). The observed soiling rate is consistent with previous studies in dry environments, which found rates between 0.1% and 1% day^{-1} (Caron and Littmann, 2013; Guo et al., 2015; Bhasker and Arya, 2015; Kazmerski et al., 2014). This soiling rate signifies the importance of regular cleaning , especially during the dry season. After sampling period A, there was only 1 minor rain event on October 29th. The influence of changing meteorological conditions on soiling is further discussed in a later section.

Gujarat, India has 1344 MW of installed PV as of 2018 (India, 2018). PV systems in this region typically have a capacity factor (actual energy generation over the installed capacity) of ~ 0.18 (Lab, 2019). The average cost of PV solar is this region is around 0.07 USD kWh^{-1} (REN21, 2018). Bergin et al. (2017), used a global climate model (GCM) and estimated that the annual soiling loss was ~ 8% in Gujarat, although this assumed monthly cleaning of the solar panels and no soiling during monsoon months. For this study, the soiling loss over a one month period was ~ 11%. This value is higher than the estimate by Bergin et al. (2017) for reasons including that it is not an annual average, represents a time of relatively high soiling and low precipitation removal, and that the Bergin et al. (2017) model estimates are likely lower limit values. The lower limit estimate of an 8% reduction in annual solar power generation equates to a yearly loss of ~ 12 million USD in Gujarat. Considering the soiling rate observed here, the magnitude of yearly loss is unavoidable without intervention by regular cleaning and/or anti-soiling coatings. Determination of the best practices for soiling prevention and remediation requires further insight into the relationship between mass loading and soiling loss (Fig. 3), as well as the size and composition of the deposited particles, which plays a role in which removal methods are most effective.

In addition to the Pearson Correlation Coefficient, the linear regression in Fig. 3 ($R^2 = 0.86$) also indicates the promising correlation between ML_{dm} estimations and SL_m. This regression also points out the linearity between ML_{dm} and SL_m for the mass loadings experienced during this field study. SL increasing proportionally to ML is consistent with previous findings (Bergin et al., 2017; Jiang et al., 2011; Boyle
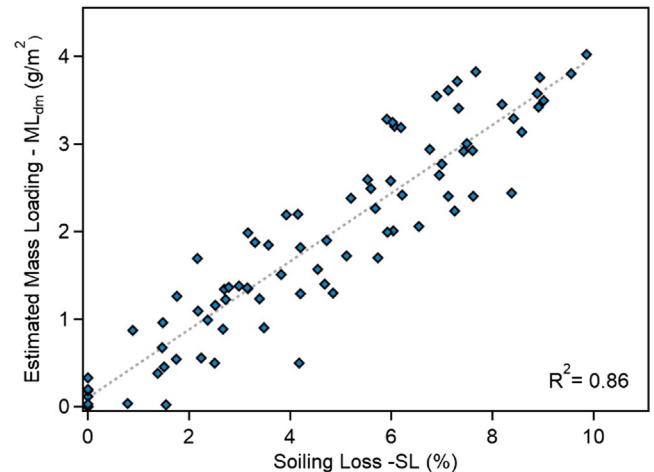

Fig. 3. MLdm (mass loading estimation from the digital microscope) and SL (soiling loss from the Campbell Scientific soiling station) values plotted for each day of this study from September 1st 2018 to January 9th 2019.

et al., 2015; Javed et al., 2017; Piedra et al., 2018). It has been observed that only under high mass loadings (> 5 g m^{-2}) will this relationship begin to show non-linearity, meaning further buildup of surface mass does not induce a proportional response in soiling loss (Mastekbayeva and Kumar, 1999).

It is worthwhile to point out that the methodology used in our image processing can change the estimation of mass loading by an order of magnitude, as seen in the sensitivity analysis performed (see Supplemental Information). The auto threshold method for this study was chosen by first manually adjusting the threshold to highlight all particles, and then choosing the auto threshold method which most closely matched the results of the manual method. It is important that the same ImageJ auto thresholding procedure and density is used throughout the study in order to create a reliable calibration curve (Fig. 3). The slope of this regression may change seasonally given the particle size distribution and composition (and thus mass loading and the particle's optical properties) has been shown to shift over seasons (Tanesab et al., 2017).

Using the linear regression equation acquired by the calibration curve (Fig. 3), we predict SL_{dm} (where the 'dm' stands for digital microscopy) from the estimated ML_{dm} values. Upon doing this, the Root-Mean-Square Deviation for the estimated versus actual soiling loss (SL_{dm} vs. SL) is found to be 1.08% soiling, equating to around $\pm$ 10% error in the upper range of observed soiling losses for this study. The system's promising accuracy shows that this tool is an excellent and low cost alternative to estimate soiling loss. There is value for using this system in both research and in industry, where soiling can vary

Table 1

Soiling loss (SL – from the Campbell Soiling Station), and measured mass loading (ML – determined from the mass of collected PM) are used to quantify the soiling loss per unit deposited mass (SL/ML). The mass loading estimated from the digital microscope (ML_{dm}) is shown along with the estimated soiling per unit deposited mass (SL/ML_{dm} – found by dividing measured soiling loss by estimated mass loading). The average Sl/ML does not include sampling period A. The average SL/ML_{dm} is the inverse slope of the linear fit of Fig. 3.

Sampling Period	Soiling Loss SL (%)	Measured Mass Loading ML ($g\,m^{-2}$)	Estimated Mass Loading ML_{dm} ($g\,m^{-2}$)	Soiling per Unit Deposited Mass SL/ML (% / $g\,m^{-2}$)	Estimated Soiling per Unit Deposited Mass SL/ML_{dm} (% / $g\,m^{-2}$)
A: Sept 1-Sept 26	4.84	0.11	0.50	43	9.67
B: Sept 26-Oct 17	9.86	2.02	4.03	4.9	2.45
C: Oct 17-Nov 7	8.95	1.84	3.76	4.8	2.37
D: Nov 7-Nov 30	9.15	1.46	3.82	6.2	2.15
E: Nov 30-Dec 19	7.50	1.56	3.61	4.8	2.07
F: Dec 19-Jan 9	7.52	1.54	2.24	4.9	3.24
Average	8.00	1.42	3.00	5.12	2.39

significantly (> 6%) across a single PV site (Gostein et al., 2013), and a network of expensive monitoring systems is not economically feasible.

Soiling loss per mass loading is an important indicator of how effectively the deposited particles can reduce PV energy production. This 'potency' of the deposited PM to soiling can vary regionally and seasonally (Bergin et al., 2017; Sayyah et al., 2014). The inverse slope of the fitted line in Fig. 3 represents the estimated soiling per mass loading (SL/ML_{dm}), which is estimated to be $2.39 \pm 1.1\%/g\,m^{-2}$. This value is underestimated, likely attributed to overestimation of the mass loading by either the image analysis technique, the deposition surface area of the system, or subtle differences in the surface properties between the digital microscope system and the soiling station panels. This value can be corrected by calibrating ML_{dm} to a measured mass loading value, ML. Measured mass loadings were determined by collecting surface PM from the soiled panel of the Campbell Scientific soiling station, which was done at the end of each of the six sampling periods. Table 1 introduces the measured ML and SL/ML values.

The method for ML_{dm} determination consistently overestimates loadings, as is evident by comparison with the measured mass loading (ML) values. The average overestimation is $1.6 \pm 0.74\,g\,m^{-2}$ and is likely the result of two factors: the LED lights shining up through the particles cause the image analysis software to overestimate the particle size, and/or groups of adjacent particles being interpreted as 1 large particle by the ImageJ software. While the mass loading is overestimated, there is a high correlation between ML_{dm} and ML (Pearson Correlation Coefficient = 0.91). This overestimation in the mass loadings creates an underestimated SL/ML_{dm}. It should be noted that the underestimation of SL/ML_{dm} by using the digital microscopy images is not surprising given the overestimation of ML by the imaging method. Given the proper comparative data (Fig. 3), ML_{dm} can be calibrated at a given location which will yield more accurate estimates of soiling loss per unit mass.

All sampling periods after the last rain event of September 22nd (B-F) have similar SL/ML values of $5.12 \pm 0.55\%/g\,m^{-2}$, consistent with findings from other studies (Boyle et al., 2015; Boyle et al., 2013; Piedra et al., 2018). This is significantly lower than SL/ML values found in Bergin et al. (2017) which found SL/ML values of 17 and 12% / $g\,m^{-2}$. The reason for this difference may be that the samples in this study and the Bergin et al. (2017) study were from a different time period which may have had a higher abundance of smaller pollution particles relative to dust. More data is needed to confirm this. The first sampling period (A) has an order-of-magnitude higher SL/ML due to the low mass loading ($0.11\,g\,m^{-2}$). This can be attributed to a heavy rain just a few days prior to the end of the sampling period. The significance of rain to soiling and mass flux to the panel surface will be discussed in a later section. To better understand the impacts of deposited PM on soiling beyond soiling per unit deposited mass, the size distribution of the deposited PM is needed.

3.2. Size dependent soiling loss estimation

Particle size and refractive index, both related to particle sources, are key factors needed to estimate the influence of light extinction (both scattering and absorption) by deposited particles and their subsequent impact on light available to solar PVs (Waggoner et al., 1981). Furthermore, size distribution of deposited PM combined with theoretical light extinction calculations allows for size dependent transmission loss, and determination of which size ranges most influence soiling (Fig. 4). Mass and soiling loss estimations resulting from sample slide analyses with optical microscopy will be referred to as ML_{om} and SL_{om}, respectively (where the 'om' subscript stands for optical microscopy). For a complete description of the methods to obtain Fig. 4, refer to the Supplemental Information.

In India, ambient PM is influenced by anthropogenic sources (i.e. trash and refuse burning/biomass burning/mobile sources/industrial emissions/construction) and natural sources (i.e. wind-blown dust) (Ram et al., 2010; Villalobos et al., 2015; Vreeland et al., 2016). The bimodal mass loading size distributions (peaks at 0.25–1 μm and 15–25 μm) seen in Fig. 4 are consistent with the expected size of most anthropogenically and most naturally sourced PM, respectively, although there are examples of large anthropogenically source and small naturally source PM particles. Larger PM particles dominate mass, with more than 90% of the deposited mass present in particles more than 10 μm, the largest of which are near 50 μm in diameter. This result points out the importance of large particles to mass loadings on panels. While larger particles dominate mass, this is not true for the estimated soiling impacts where more than 50% of the soiling is from particles less than 5 μm in diameter. This is consistently observed across the study as seen in the top parts of each plot in Fig. 4, where small particles dominate soiling losses. Mass and soiling distributions appear to remain similar throughout the study. We confirm this by using a two sample Kolmogorov-Smirnov test ($\alpha = 0.01$) to test if the distributions are statistically similar throughout the study. This test was performed between each of the mass distributions (i.e. each sampling period's mass distribution was tested against every other sampling period's mass distribution). This same procedure is done for particle size distribution of the soiling. We find that there is no significant difference between any of the distributions for both mass and soiling loss. Further analysis into how distributions change over seasons (i.e. comparing the summer month distributions with monsoon season distributions) should be considered in future studies.

These results highlight that mass loading alone cannot be used as a measure of soiling, and particle size needs to be considered. In regards to cleaning considerations, these small particles have been shown to be difficult to remove by dry cleaning alone (Ilse et al., 2018). With water scarcity a concern for many areas in India, the difficulty in cleaning small particles without water represents another challenge to the renewable energy goals of the country. If these goals are to be met, it is important to consider the sources of the PM that most influence soiling.
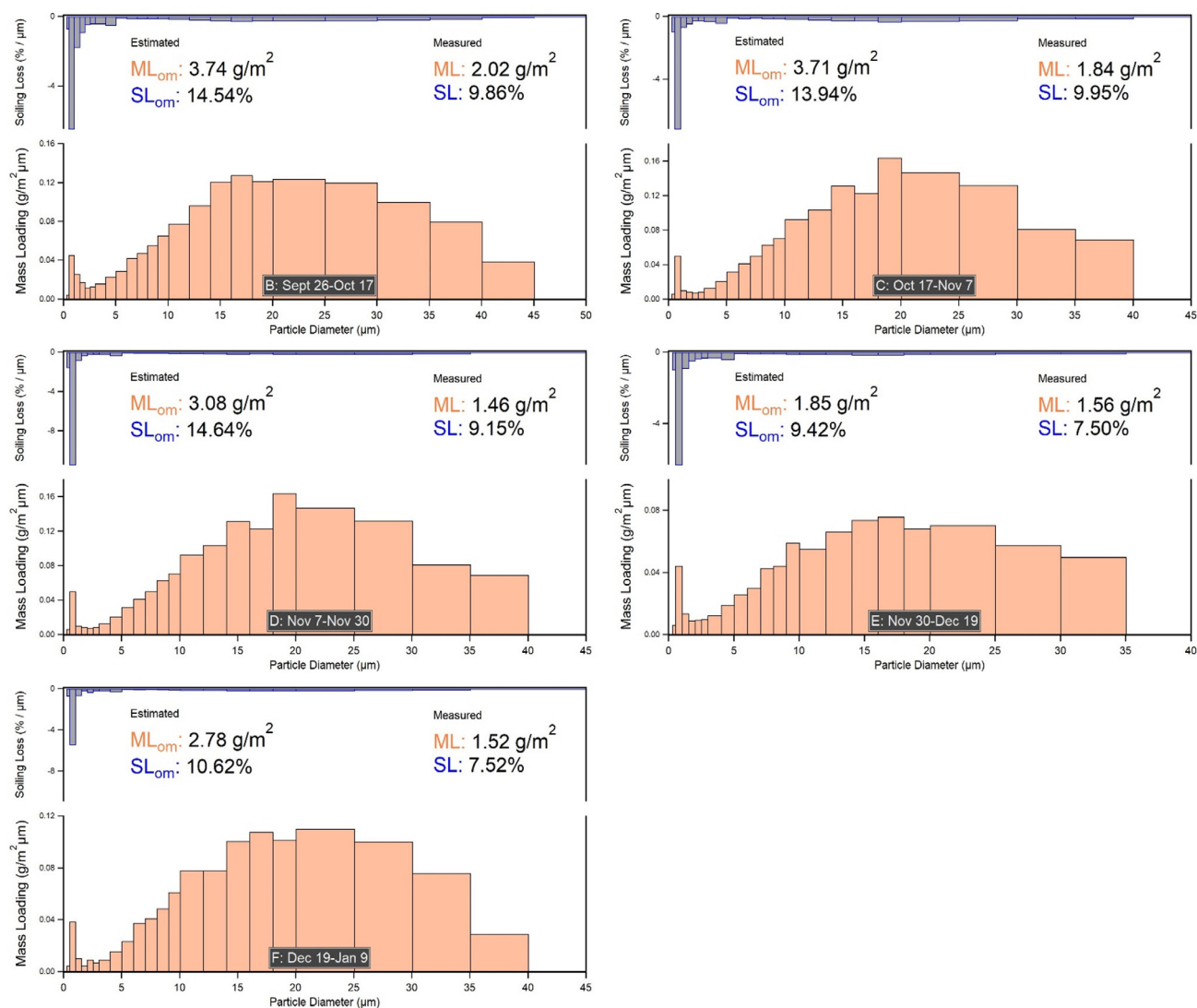
Fig. 4. Mass loading (filled tan bars) is shown as a function of particle size for each sampling period. The plots have been normalized to bin size. SLom as a function of size (shown in the upper part of each graph in grey) highlight the importance of small particles to soiling loss.

Reducing deposition of wind-blown dust which is capable of traveling over hundreds of kilometers (Ram et al., 2010; Valerino et al., 2017) is extremely difficult, however decreases in emissions of anthropogenic aerosols (typically < 5 μm in diameter) can have positive impacts to achieving India's renewable energy goals. The results also suggest that any surface technology designed to mitigate soiling needs to be able to influence a wide range of particle sizes and chemical properties.

Similarly to ML_{dm} discussed earlier, ML_{om} overestimates measured loadings by 80% ± 31% (1.36 ± 0.55 g/m^{-2}), although this may be corrected using measured values. The normalized root mean square error between ML and ML_{om} was found to be 27%. The overestimation is likely a result of the aggressive nature of the image analysis technique which can interpret some aggregated smaller particles as larger ones (see Supplemental Information for error and estimation analysis). Another possible reason for mass loading overestimation is due to differences in soiling properties of the glass slide and the soiling station panels. Finally, the assumptions used for theoretical soiling loss calculations may not be accurate. As discussed in the methods section, the inputs to the theoretical soiling calculations (spherical particle assumption, refractive index, density, absorption efficiency) are from past findings in the region (Pandithurai et al., 2008; Hu et al., 2012; Yang et al., 2009; Xu et al., 2002). More work is needed to determine the validity of these assumptions with respect to particles with non-uniform compositions.

While there may be error associated with the theoretical soiling loss calculations, the theoretical soiling loss per unit mass (SL_{om}/ML_{om}) is within 1% g^{-1} m^{-2} of the measured SL/ML (4.23 ± 0.51% / g m^{-2} and 5.26 ± 0.54% / g m^{-2}, respectively). The overestimation in the ML_{om} is not reflected in the estimated SL_{om}/ML_{om} because the estimated SL_{om} is calculated from ML_{om} (Eq. (2)), thus the overestimation is canceled out. This indicates that the image analysis procedure combined with the optical model can accurately predict soiling loss per unit deposited mass. It should be noted that the magnification used to acquire images can significantly impact the mass and soiling estimations and distributions. This method should only be applied to images with similar magnification and resolution (μm per pixel) as this study. More information on error due to using lower magnifications can be seen in the Supplementary Information. The precision of the mass estimations and accuracy of SL_{om}/ML_{om} indicate the value of optical microscopy for soiling analyses.

3.3. Influence of meteorology on soiling

Western India's monsoon season is typically from July to September. The first sampling period (A: September 1st to September 26th) fell within the monsoon season and there was 10 separate rain events over

this period. Rain events over 8 mm per hour restored the soiled panel to less than 1% soiling which is consistent with soiling restoration by rain observed in previous studies (Hammond et al., 1997; Appels et al., 2012; Haeberlin and Graf, 1998; Ryan et al., 1989). Light rain events (< 5 mm hour^{-1}) did not fully restore soiled panels, as is evident in Fig. 1. More data is needed in this region to confirm the threshold for panel cleaning by rain.

The rain events in sampling period A were accompanied by an average relative humidity (RH) $\sim 50\%$ higher than the other sampling periods (74% vs. 50%). This light rain and high humidity in sampling period A lead to a soiling rate twice as high as the following sampling periods B-F (0.83 $\pm$ 0.22% day^{-1} and 0.41 $\pm$ 0.04% day^{-1} respectively). It is likely that the high RH increases PM adherence to the panel surface (Mekhilef et al., 2012; Touati et al., 2012; Hoffman and Maag, 1980). Particle swelling and water absorption due to high RH have also been shown to increase soiling (Mekhilef et al., 2012). These results point out the significance that light rain and high RH can have to soiling rates, though more work should be done to confirm these results given the limited data. Another effect of rain and RH observed during sampling period A is surface cementation.

Microscopy images of slide samples present during rain events (Fig. 5A–D) shows evidence of cementation. The formation of water spots, the edge of which can be seen in Fig. 5A, and crystalline structures (Fig. 5B–D) have been observed as a result of cementation in other studies (Ilse et al., 2016; Ilse et al., 2018). Other evidence of cementation includes the presence of needle like structures (Fig. 5B,C) which are likely clay minerals (Ilse et al., 2016), as well as precipitated salts (Fig. 5B,D).

Cementation made cleaning difficult, which is a documented effect (Mekhilef et al., 2012; Bethea et al., 1981; Sayyah et al., 2014). Another impact of cementation is seen in the soiling per unit deposited mass (SL/ML) observed during the first sampling period ($\sim 40\%$/g m^{-2}). This SL/ML is an order of magitude higher than the rest of the study. Although more work needs to be done on the impacts of light rain to size distribution, it may be that rain preferentially cleans off larger (> 10 μm) particles, which has been seen in previous studies (Roth and Anaya, 1980; Appels et al., 2012). The smaller particles remaining on the surface (which are capable of greater SL/ML), explain why the SL/ML was larger during sampling period A. Assumptions of PM removal by rain need to be more carefully considered when determing cleaning schedules in India. The influence of RH on soiling rate also needs to be considered when estimating future soiling impacts at a site.
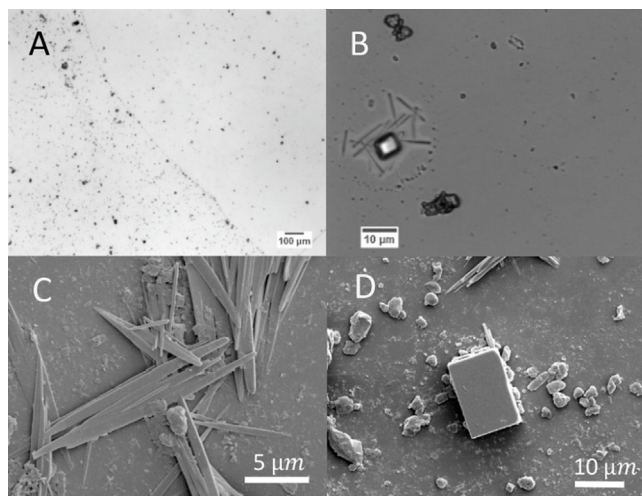

Fig. 5. Panel A shows the edge of an evaporated water droplet on a glass slide at 5x magnification. B shows this same sample imaged at 40x magnification, indicating crystalline structures left behind from the evaporated drop. C and D are scanning electron microscope images showing some crystal structures present on the slides.

Another key variable that has historically been considered an import influence on soiling is ambient PM concentrations, which are a proxy for PM dry deposition fluxes. Other studies have shown mixed results regarding the positive relationship between soiling and ambient PM (Guo et al., 2015; Fountoukis et al., 2018; Figgis et al., 2016; Micheli and Muller, 2017). In this study, there was no significant relationship between soiling rates and ambient PM$_{10}$ concentrations even though ambient PM$_{10}$ increased throughout the study. The average PM$_{10}$ concentration was 2.5 times *higher* in the dry period (112 μg m^{-3} vs. 42 μg m^{-3}), but soiling rate was 2 times *lower*. While ambient PM$_{10}$ concentrations did not impact soiling rates, it was a factor in the observed effective deposition velocity (Figgis et al., 2016) (cm s^{-1}), which was found by dividing the PM accumulation flux (μg cm^{-2} s^{-1}) by the ambient PM$_{10}$ concentration (μg cm^{-3}). In the rainy period the effective deposition velocity (v_d) was between 3 and 4 cm s^{-1}. Effective v_d during the dry period dropped by 5 to 10 times that of the rainy period to between 0.4 and 1 cm s^{-1}. While caution should be taken in extrapolating this limited data set, it is hypothesized this is due to higher RH, which has been shown to increase v_d for both large and small particles (Winkler, 1974; Isaifan et al., 2019). The relationship of RH and ambient PM concentration is further discussed in the Supplemental Information. Another possible reason for the dramatic range in observed effective v_d is a change in windspeed. Previous studies have shown a positive correlation between particle deposition and windspeed, (Bhattacharya et al., 2014; Figgis et al., 2016; Goossens and Van Kerschaever, 1999), however no such correlation was found in this study using daily average windspeed and daily mass loading increase as estimated by the digital microscope system. Although more data is needed, impacts of rain and RH may be a contributing factor for the inability to use ambient PM as an indicator of soiling rate and it is not recommended that PM$_{10}$ be used as a sole predictor of soiling in India.

3.4. Module temperature as a component of soiling

The temperature of a PV module has an inverse relationship with efficiency. Most polycrystalline panels, including those used in this study, have a 0.5% decrease in efficiency for every 1 °C above 25 °C (as per manufacture specifications). For a majority of the study, the soiled panel was cooler than the reference by an average of 1.2 $\pm$ 1.0 °C. This equates to the soiled panel being around 0.5% more efficient than the reference panel (based on temperature considerations alone). The lower temperature of the soiled panel served to mask some of the impacts of soiling. If the temperature effect was considered in the SL calculations (Eq. (1)), the soiling ratio would increase by $\sim 0.5\%$ on average. It may be that the observed temperature difference is due to soiling which has been observed in previous studies as a result of uniform soiling (Schill et al., 2015). It is also possible that other factors contributed to this difference in temperature (i.e. panel hot spots, uneven convective cooling etc.). More work should be done regarding the impact of soiling to panel temperature.

4. Conclusions

Using a reference soiling station, a low cost digital microscope system has been validated as a inexpensive alternative to monitoring PV soiling. When a linear calibration between ML$_{dm}$ and SL was applied, the system was able to estimate soiling losses (SL$_{dm}$) to within 1% soiling. Soiling losses continued to increase at a rate of 0.37% day^{-1} throughout this study. Using this information, a 10% PV energy loss (which is a conservative estimation) costs the state of Gujarat 12 million USD per year. These losses are due to a combination of anthropogenic PM and natural dust, the combination of which reduces energy production by $\sim 5\%$ per g m^{-2} of deposited matter. Using a new optical microscopy and image analysis method combined with a new theoretical model, it has been shown that $> 90\%$ of the deposited mass is from particles > 10 μm in diameter. While large particles dominate

mass, > 50% of soiling impacts are from particles < 5 µm in diameter. This suggests that PV energy in India could greatly benefit from reductions in anthropogenic PM emissions. It is also recommended that cleaning methods, and work on possible intervention by surface coatings, should focus on the removal of small particles. In regards to natural cleaning, the threshold for cleaning by rain was found to be 8 mm hour^{-1}. Rainy periods in India are accompanied by higher RH which is shown here to increase soiling rate by 2x. Although high RH is usually accompanied by a lower ambient PM, deposition velocity of this PM to the panel surface is 5-10x higher compared to dry periods. It is not recommended that ambient PM be used as a predictor of soiling in India, and RH may be a better predictor of soiling rates.

Declaration of Competing Interest

The authors declare that they have no known competing financial interests or personal relationships that could have appeared to influence the work reported in this paper.

Acknowledgements

Appendix A. Supplementary data

Supplementary data to this article can be found online at https://doi.org/10.1016/j.solener.2020.03.118.

References

Abu-Naser, M., 2017. Solar panels cleaning frequency for maximum financial profit. Open J. Energy Efficiency 06 (03), 80–86.

Appels, R., Muthirayan, B., Beerten, A., Paesen, R., Driesen, J., Poortmans, J., 2012. The effect of dust deposition on photovoltaic modules, in: IEEE (Ed.) Photovoltaic Specialists Conference (PVSC).

Baras, A., Jones, R.K., Alqahtan, A., Alodan, M., 2016. Measured Soiling Loss and its Economic Impact for PV Plants in Central Saudi Arabia. Smart Grid (SASG) Saudi Arabia.

Bergin, M.H., Ghoroi, C., Dixit, D., Schauer, J.J., Shindell, D.T., 2017. Large reductions in solar energy production due to dust and particulate air pollution. Environ. Sci. Technol. Lett. 4 (8), 339–344.

Bethea, R.M., Barriger, M.T., Williams, P.F., Chin, S., 1981. Environmental effects on solar concentrator mirrors. Sol. Energy 27 (6), 497–511.

Bhasker, V., Arya, R., 2015. Effects of natural dust on the performance of solar PV panel in India. J. Energy Environ. Carbon Credits 5 (2), 1–6.

Boyle, L., Flinchpaugh, H., Hannigan, M.P., 2013. Impact of natural soiling on the transmission of PV cover plates, Photovoltaic Specialists Conference (PVSC).

Boyle, L., Flinchpaugh, H., Hannigan, M.P., 2015. Natural soiling of photovoltaic cover plates and the impact on transmission. Renewable Energy 77, 166–173.

Caron, J.R., Littmann, B., 2013. Direct monitoring of energy lost due to soiling on first solar modules in California. IEEE J. Photovoltaics 3 (1), 336–340.

Cuddihy, E.F., 1980. Theoretical considerations of soil retention. Solar Energy Mater. 3, 21–33.

Dobaria, B., Pandya, M., Aware, M., 2016. Analytical assessment of 5.05 kWp grid tied photovoltaic plant performance on the system level in a composite climate of western India. Energy 111, 47–51.

Dolan, D., Prodanov, V., Taufik, T., 2015. Energy and economic losses due to soiling on utility scale PV system to guide timing of cost effective cleaning, in: IEEE (Ed.) Photovoltaic Specialist Conference (PVSC), 42.

El-Shobokshy, M.S., Hussein, F.M., 1992. Degradation of photovoltaic cell performance due to dust deposition on to its surface. Renewable Energy 3, 585–590.

Figgis, B., Ennaoui, A., Guo, B., Javed, W., Chen, E., 2016. Outdoor soiling microscope for measuring particle deposition and resuspension. Sol. Energy 137, 158–164.

Fountoukis, C., Figgis, B., Ackermann, L., Ayoub, M.A., 2018. Effects of atmospheric dust deposition on solar PV energy production in a desert environment. Sol. Energy 164, 94–100.

Goossens, D., 2005. Quantification of the dry aeolian deposition of dust on horizontal surfaces: an experimental comparison of theory and measurements. Sedimentology 52 (4), 859–873.

Gostein, M., Littmann, B., Caron, R., Dunn, L., 2013. Comparing PV power plant soiling

measurements extracted from PV module irradiance and power measurements, Photovoltaic Specialists Conference (PVSC).

Guo, B., Javed, W., Figgis, B., Mirza, T., 2015. Effect of dust and weather conditions on photovoltaic performance in Doha, Qatar. First Workshop on Smart Grid and Renewable Energy (SGRE), IEEE.

Haeberlin, H., Graf, J.D., 1998. Gradual reduction of PV generator yield due to pollution, 2nd World Conference on Photovoltaic Solar Energy Conversion. Austria, Vienna.

Hammond, R., Srinivasa, D., Harris, A., Whitfield, K., 1997. Effects of soiling on PV module and radiometer performance, Photovoltaic Specialists Conference, Conference Record of the Twenty-Sixth. IEEE.

Hoffman, A.R., Maag, C.R., 1980. Photovoltaic module soiling studies, May 1978-October 1980, in: Energy, U.D.o. (Ed.). Jet Propulsion Laboratory Pasadena, California.

Hu, M., Peng, J., Sun, K., Yue, D., Guo, S., Wiedensohler, A., Wu, Z., 2012. Estimation of size-resolved ambient particle density based on the measurement of aerosol number, mass, and chemical size distributions in the winter in Beijing. Environ. Sci. Technol. 46 (18), 9941–9947.

Ilse, K., Werner, M., Naumann, V., Figgis, B.W., Hagendorf, C., Bagdahn, J., 2016. Microstructural analysis of the cementation process during soiling on glass surfaces in arid and semi-arid climates. Phys. Status Solidi (RRL) - Rapid Res. Lett. 10 (7), 525–529.

Ilse, K.K., Figgis, B.W., Werner, M., Naumann, V., Hagendorf, C., Pöllmann, H., Bagdahn, J., 2018. Comprehensive analysis of soiling and cementation processes on PV modules in Qatar. Sol. Energy Mater. Sol. Cells 186, 309–323.

India, G.o., 2018. Annual report, in: Energy, M.o.N.a.R. (Ed.). Goverment of India.

Isaifan, R.J., Johnson, D., Ackermann, L., Figgis, B., Ayoub, M., 2019. Evaluation of the adhesion forces between dust particles and photovoltaic module surfaces. Sol. Energy Mater. Sol. Cells 191, 413–421.

Javed, W., Wubulikasimu, Y., Figgis, B., Guo, B., 2017. Characterization of dust accumulated on photovoltaic panels in Doha, Qatar. Sol. Energy 142, 123–135.

Jiang, H., Lu, L., Sun, K., 2011. Experimental investigation of the impact of airborne dust deposition on the performance of solar photovoltaic (PV) modules. Atmos. Environ. 45 (25), 4299–4304.

Jones, R.K., Baras, A., Saeeri, A.A., Al Qahtani, A., Al Amoudi, A.O., Al Shaya, Y., Alodan, M., Al-Hsaien, S.A., 2016. Optimized cleaning cost and schedule based on observed soiling conditions for photovoltaic plants in central Saudi Arabia. IEEE J. Photovoltaics 6 (3), 730–738.

Kazmerski, L.L., Al Jardan, M., Al Jnoobi, Y., Al Shaya, Y., John, J.J., 2014. Ashes to ashes, dust to dust: averting a potential showstopper for solar photovoltaics, in: IEEE (Ed.) 2014 IEEE 40th Photovoltaic Specialist Conference.

Khan, G., Rathi, S., 2014. Optimal site selection for solar PV power plant in an indian state using geographical information system (GIS). Int. J. Emerg. Eng. Res. Technol. 2 (7), 260–266.

Lab, N.R.E., 2019 National Solar Radiation Database https://maps.nrel.gov/nsrdb-viewer/.

Laven, P., 2018. MiePlot v4.6.14 ed., p. Computer Program for Scattering of Light From a Sphere Using Mie Theory & the Debye Series.

Mahtta, R., Joshi, P., Jindal, A.K.J.R.e., 2014. Solar power potential mapping in India using remote sensing inputs and environmental parameters. 71, 255–262.

Mastekbayeva, G.A., Kumar, S., 1999. Effect of dust on the transmittance of low density polyethylene glazing in a tropical climate. Sol. Energy 68 (2), 135–141.

Mekhilef, S., Saidur, R., Kamalisarvestani, M., 2012. Effect of dust, humidity and air velocity on efficiency of photovoltaic cells. Renew. Sustain. Energy Rev. 16 (5), 2920–2925.

Micheli, L., Muller, M., 2017. An investigation of the key parameters for predicting PV soiling losses. Prog. Photovoltaics Res. Appl. 25 (4), 291–307.

Mie, G., 1908. Pioneering mathematical description of scattering by spheres. Ann. Phys. 25, 337.

Mishchenko, M.I., Travis, L.D., Kahn, R.A., West, R.A., 1997. Modeling phase functions for dustlike tropospheric aerosols using a shape mixture of randomly oriented polydisperse spheroids. J. Geophys. Res.: Atmos. 102 (D14), 16831–16847.

Padmavathi, K., Daniel, S.A., 2013. Performance analysis of a 3MWp grid connected solar photovoltaic power plant in India. Energy Sustain. Dev. 17 (6), 615–625.

Pandithurai, G., Dipu, S., Dani, K.K., Tiwari, S., Bisht, D.S., Devara, P.C.S., Pinker, R.T., 2008. Aerosol radiative forcing during dust events over New Delhi, India. J. Geophys. Res. 113 (D13).

Piedra, P.G., Llanza, L.R., Moosmüller, H., 2018. Optical losses of photovoltaic modules due to mineral dust deposition: experimental measurements and theoretical modeling. Sol. Energy 164, 160–173.

Ram, K., Sarin, M.M., Tripathi, S.N., 2010. A 1 year record of carbonaceous aerosols from an urban site in the Indo-Gangetic Plain: characterization, sources, and temporal variability. J. Geophys. Res.: Atmos. 115 (D24).

Ramachandra, T.V., Jain, R., Krishnadas, G., 2011. Hotspots of solar potential in India. Renew. Sustain. Energy Rev. 15 (6), 3178–3186.

REN21, 2018. Renewables 2018 Global Status Report.

Roth, E.P., Pettit, R.B., 1980. The Effect of Soiling on Solar Mirrors and the Techniques Used to Maintain High Reflectivity. Alburquerque, New Mexico.

Ryan, C.P., Vignola, F., McDaniels, D.K., 1989. Solar cell arrays: degradation due to dirt. In: Proceedings of the American Section of the International Solar Energy Society, pp. 234–237.

Sayyah, A., Horenstein, M.N., Mazumder, M.K., 2014. Energy yield loss caused by dust deposition on photovoltaic panels. Sol. Energy 107, 576–604.

Schill, C., Brachmann, S., Koehl, M., 2015. Impact of soiling on IV -curves and efficiency of PV-modules. Sol. Energy 112, 259–262.

Schindelin, J., Arganda-Carreras, I., Frise, E., Kaynig, V., Longair, M., Pietzsch, T., Preibisch, S., Rueden, C., Saalfeld, S., Schmid, B., Tinevez, J.Y., White, D.J., Hartenstein, V., Eliceiri, K., Tomancak, P., Cardona, A., 2012. Fiji: an open-source

platform for biological-image analysis. Nat. Methods 9 (7), 676–682.

Sharma, V., Chandel, S.J.S.E., 2016. A novel study for determining early life degradation of multi-crystalline-silicon photovoltaic modules observed in western Himalayan Indian climatic conditions. Sol. Energy 134, 32–44.

Shukla, A.K., Sudhakar, K., Baredar, P., 2016. Simulation and performance analysis of 110 kWp grid-connected photovoltaic system for residential building in India: a comparative analysis of various PV technology. Energy Rep. 2, 82–88.

Sundaram, S., Babu, J.S.C.J.E.c., management, 2015. Performance evaluation and validation of 5 MWp grid connected solar photovoltaic plant in South India. 100, 429–439.

Tanesab, J., Parlevliet, D., Whale, J., Urmee, T., 2017. Seasonal effect of dust on the degradation of PV modules performance deployed in different climate areas. Renewable Energy 111, 105–115.

Tanesab, J., Parlevliet, D., Whale, J., Urmee, T., 2018. Energy and economic losses caused by dust on residential photovoltaic (PV) systems deployed in different climate areas. Renewable Energy 120, 401–412.

Touati, F., Al-Hitmi, M., Bouchech, H., 2012. Towards Understanding the Effects of Climatic and Environmental Factors on Solar PV Performance in Arid Desert Regions (Qatar) for Various PV Technologies, International Conference on Renewable Energies and Vehicular Technology. IEEE.

Valerino, M.J., Johnson, J.J., Izumi, J., Orozco, D., Hoff, R.M., Delgado, R., Hennigan, C.J., 2017. Sources and composition of PM2.5 in the Colorado Front Range during the DISCOVER-AQ study. J. Geophys. Res.: Atmos. 122 (1), 566–582.

Villalobos, A.M., Amonov, M.O., Shafer, M.M., Devi, J.J., Gupta, T., Tripathi, S.N., Rana,

K.S., McKenzie, M., Bergin, M.H., Schauer, J.J., 2015. Source apportionment of carbonaceous fine particulate matter (PM 2.5) in two contrasting cities across the Indo-Gangetic Plain. Atmos. Pollut. Res. 6 (3), 398–405.

Vreeland, H., Schauer, J.J., Russell, A.G., Marshall, J.D., Fushimi, A., Jain, G., Sethuraman, K., Verma, V., Tripathi, S.N., Bergin, M.H., 2016. Chemical characterization and toxicity of particulate matter emissions from roadside trash combustion in urban India. Atmos. Environ. 147, 22–30.

Waggoner, A.P., Weiss, R.E., Ahlquist, N.C., Covert, D.S., Will, S., Charlson, R.J., 1981. Optical characteristics of atmospheric aerosols atmospheric environment 15, 1891–1909.

Winkler, P., 1974. Relative humidity and the adhesion of atmospheric particles to the plates of impactors. J. Aerosol Sci. 5 (3), 235–240.

Wiscombe, W.J., Grams, G.W., 1976. The backscattered fraction in two-stream approximations. J. Atmos. Sci. 33.

Xu, J., Bergin, M.H., Yue, X., Liu, G., Zhao, J., Carrico, C.M., Baumann, K., 2002. Measurement of aerosol chemical, physical and radiative properties in the Yangtze delta region of China. Atmos. Environ. 36, 161–173.

Yang, M., Howell, S.G., Zhuang, J., Huebert, B.J., 2009. Attribution of aerosol light absorption to black carbon, brown carbon, and dust in China – interpretations of atmospheric measurements during EAST-AIRE. Atmos. Chem. Phys.

Zheng, T., Bergin, M.H., Johnson, K.K., Tripathi, S.N., Shirodkar, S., Landis, M.S., Sutaria, R., Carlson, D.E., 2018. Field evaluation of low-cost particulate matter sensors in high- and low-concentration environments. Atmos. Meas. Tech. 11 (8), 4823–4846.